PHYSICAL REVIEW B **91**, 201106(R) (2015)

Classification of collective modes in a charge density wave by momentum-dependent modulation of the electronic band structure

D. Leuenberger,[1,2] J. A. Sobota,[1,2,3] S.-L. Yang,[1,2,4] A. F. Kemper,[3] P. Giraldo-Gallo,[1,2] R. G. Moore,[1,2] I. R. Fisher,[1,2] P. S. Kirchmann,[1,*] T. P. Devereaux,[1,2] and Z.-X. Shen[1,2,4,†]

[1]*Stanford Institute for Materials and Energy Sciences, SLAC National Accelerator Laboratory, 2575 Sand Hill Road, Menlo Park, California 94025, USA*

[2]*Department of Applied Physics, Geballe Laboratory for Advanced Materials, Stanford University, Stanford, California 94305, USA*

[3]*Lawrence Berkeley National Laboratory, 1 Cyclotron Road, Berkeley, California 94720, USA*

[4]*Department of Physics, Stanford University, Stanford, California 94305, USA*

(Received 5 December 2014; revised manuscript received 1 May 2015; published 21 May 2015)

We present time- and angle-resolved photoemission spectroscopy (trARPES) measurements on the charge density wave system $CeTe_3$. Optical excitation transiently populates the unoccupied band structure and reveals a gap size of $2\Delta = 0.59$ eV. The occupied Te-5p band dispersion is coherently modified by three modes at $\Omega_1 = 2.2$, $\Omega_2 = 2.7$, and $\Omega_3 = 3$ THz. All three modes lead to small rigid energy shifts whereas Δ is only affected by Ω_1 and Ω_2. Their spatial polarization is analyzed by fits of a transient model dispersion and density-functional theory frozen phonon calculations. We conclude that modes Ω_1 and Ω_2 result from in-plane ionic lattice motions, which modulate the charge order and that Ω_3 originates from a generic out-of-plane A_{1g} phonon. We thereby demonstrate how the rich information from trARPES allows identification of collective modes and their spatial polarization, which explains the mode-dependent coupling to charge order.

DOI: 10.1103/PhysRevB.91.201106 PACS number(s): 78.47.J−, 63.20.kd, 71.45.Lr, 73.20.Mf

Interaction of multiple degrees of freedom in quantum materials can result in ordering phenomena that give rise to complex phase diagrams with competing or intertwined orders [1]. Such broken-symmetry ground states host characteristic low-energy excitations, which are intimately related to the interactions responsible for ordering. Ultrafast nonequilibrium methods are a new and active field for the investigation of broken-symmetry phases as they grant direct access to collective modes in the time domain [2–7] and can provide strong evidence for the ordering mechanism operating in a particular material [8,9].

Charge density wave (CDW) formation is one of the most basic and widely studied cases for long-range ordering when only electronic and lattice degrees of freedom are interacting [10]. Below a critical temperature T_{CDW} a spontaneous lattice distortion Δz appears, generally originating via the complex interplay of the electronic structure and lattice. This results in a spatial charge modulation at a wave vector $\vec{q}$ (spatial period $2\pi/q$) and opening of a band gap 2Δ in the band structure, which minimizes the system's total energy by reducing the kinetic energy of the electronic system. One of the characteristic collective excitations in such Peierls-like CDWs is a gapped amplitude mode (AM), which modulates the magnitude $\Delta(t)$ of the order parameter [10].

Quasi-two-dimensional (2D) rare-earth tritellurides RTe_3 (R = Y,La-Sm,Gd-Tm) form an incommensurate CDW along the crystallographic c axis and have been studied extensively [11–19]. At low temperatures, the heaviest members of the RTe_3 series (R = Dy-Tm) additionally order with a second CDW perpendicular to the first CDW [15,19,20]. Angle-resolved photoemission spectroscopy (ARPES) reveals the Fermi-surface (FS) topology and the momentum-dependent gap structure [20–24].

Collective modes in RTe_3 were studied with Raman spectroscopy [19,25,26], time-resolved optical reflectivity [7,27,28], and time-resolved ARPES (trARPES) [4,29,30]. Yet even for this thoroughly investigated CDW system unambiguous identification of an AM is nontrivial. Lowering the translational symmetry in the CDW phase leads to the renormalization of the normal-state optical and acoustic phonon branches at $\vec{q}$ [25–27]. Ubiquitously observed generic phonon modes add to the difficulty of mode identification. Direct comparison of modes observed in the CDW phase to the calculated phonon spectra is hampered by the incommensurable CDW in RTe_3. These challenges are present in CDW materials in general and have led to conflicting reports regarding the AM in RTe_3 in particular. In $DyTe_3$, for instance, a 1.75-THz mode is observed in temperature-dependent transient reflectivity [27], Raman spectroscopy [26], and a trARPES experiment using a pump-pump-probe scheme [30]. Optical measurements attribute this mode to a phonon in the lower symmetry CDW state that is coupled to the AM, whereas trARPES [30] assigns it to a second AM.

In this Rapid Communication, we report a trARPES study of the collective response of $CeTe_3$ in the CDW phase. The unoccupied band structure is transiently populated by optical transitions, which reveals a gap size of $2\Delta = 0.59(2)$ eV. The occupied Te-5p band dispersion near the CDW gap is coherently modified by three modes and analyzed within a transient tight-binding (TB) model. Momentum-dependent analysis combined with density-functional theory (DFT) frozen phonon calculations reveals different coupling to the band structure for in-plane AMs and out-of-plane optical phonons.

*kirchman@stanford.edu
†zxshen@stanford.edu

Small rigid shifts in the band dispersion E_0 are introduced by all three modes, whereas much larger periodic modulations of Δ are driven by lattice motions $\Omega_1 = 2.2$ and $\Omega_2 = 2.7$ THz. We explain this observation by concluding that both modes Ω_1 and Ω_2 result from in-plane ionic motions which are coupled to the CDW and hence drive oscillations of Δ as AMs. The $(\Omega_3 = 3)$-THz mode originates from an out-of-plane optical A_{1g} phonon that does not couple to the CDW. Our work demonstrates how careful evaluation of the rich information from trARPES allows unambiguous identification of AMs in charge-ordered materials.

Our trARPES setup [31,32] consists of an amplified laser system operating at a 310-kHz repetition rate that drives an optical parametric amplifier to optically excite the sample with ∼50-fs pump pulses at a photon energy of 1.03 eV. Electrons are photoemitted with ∼150-fs probe pulses at 6 eV as a function of pump-probe delay and collected with 50-fs delay steps in a hemispherical electron analyzer, yielding a total energy resolution of ∼22 meV. $CeTe_3$ single crystals were grown by slow cooling of a binary melt [14]. Measurements were performed on freshly cleaved $CeTe_3$ samples at $T = 100$ K in an ultra-high-vacuum chamber with a pressure of $<1 \times 10^{-10}$ torr. Phonon eigenmodes of the normal state of RTe_3 were calculated from the dynamical matrix using the QUANTUM-ESPRESSO [33] package with ultrasoft pseudopotentials and the Perdew-Burke-Ernzerhof [34] exchange-correlation functional, a kinetic-energy cutoff of 500 eV, and $13 \times 3 \times 13$ k points. Incident pump fluences of 55–354 μJ/cm^2 correspond to absorbed energies of 16–103 meV per unit cell at the surface, see Supplemental Material [35]. The value of 2Δ decreases by no more than 15%, and the system responds linearly, see Supplemental Material [35], without melting of the charge order. This is in contrast to previous studies at higher excitation densities [4,29,30] where qualitative changes in the dispersion prevent decoupling the effects of coherent in-plane and out-of-plane motions.

Figure 1(b) illustrates the cut through the FS where the trARPES data, which are shown in Figs. 1(c) and 1(d) for selected pump-probe delays, have been taken. Due to an asymmetric band dispersion and a slightly curved cut in the $\vec{k} = \{k_x, k_z\}$ plane the Fermi momentum k_F does not exactly coincide with the maximum (minimum) position of the occupied (unoccupied) band. For simplicity, dispersions along $\vec{k}$ are projected on k_x. At a pump-probe delay of -330 fs the Te-5p band with the occupied part of the CDW gap is observed in equilibrium. At -25 fs, the leading edge of the pump pulse promotes electrons into unoccupied Te-5p states without yet changing the band dispersion significantly, which occurs at later delays. The magnitude of the full CDW gap $2\Delta = 0.59(2)$ eV is directly given by the difference of the maximum of the lower band at $E - E_F = -0.16(1)$ eV and the minimum of the upper band at $E - E_F = 0.43(1)$ eV. This is in agreement with previous results from optical reflectivity [13,16] whereas being smaller than extracted from ARPES [22] and larger than estimated by tunneling experiments [17].

To obtain a quantitative description of the electronic bands near E_F we consider a TB model of the in-plane Te-5$p_{x/z}$ orbitals [19,24] as sketched in Fig. 1(a). Nesting of the metallic

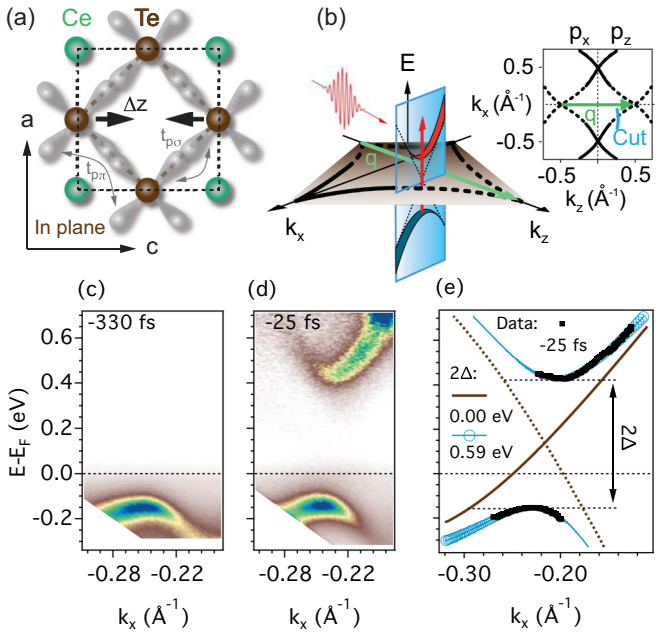

FIG. 1. (Color online) (a) Structure of the Te planes where the CDW forms along the c axis with lattice displacement Δz indicated. The FS is described in a TB model with the overlap integrals $t_{p\sigma}$ along and $t_{p\pi}$ perpendicular to the Te-5p orbitals. (b) Cartoon of the trARPES experiment on $CeTe_3$ in the CDW region of the FS (*dotted lines*). The *blue plane* illustrates an energy versus momentum cut with Te-5p bands and a pump pulse exciting electrons into unoccupied states. The *blue line* indicates the momentum cut in the experiment across the gapped region (*dotted lines*) of the calculated 2D FS, and the *green arrow* denotes the CDW wave vector $\vec{q}$. trARPES spectra for selected pump-probe delays, (c) 330 fs before the arrival of the pump pulse and (d) during the presence of the pump pulse. Intensities are rescaled exponentially as a function of energy for enhanced visibility of the transiently occupied features above E_F. (e) TB fit (*blue markers*) according to Eqs. (1) and (2) to the extracted band dispersion (*black markers*) at -25 fs yields $2\Delta = 0.59(2)$ eV. The size of the *blue markers* is proportional to the calculated spectral weight of the TB bands [24]. The *brown lines* indicate the calculated metallic bare band dispersion.

bare bands $\epsilon(\vec{k})$ via $\vec{q}$ creates two branches $E_{1,2}(\vec{k})$, which are separated by 2Δ [10],

$$E_{1,2}(\vec{k}) = \frac{\epsilon_{\vec{k}} + \epsilon_{\vec{k}-\vec{q}}}{2} \pm \sqrt{\left(\frac{\epsilon_{\vec{k}} - \epsilon_{\vec{k}-\vec{q}}}{2}\right)^2 + \Delta^2}. \quad (1)$$

$\epsilon(\vec{k})$ is approximated by a noninteracting TB model [19,24] of the in-plane Te-5p orbitals, see Fig. 1(a),

$$\epsilon(\vec{k}) = -2t_{p\sigma}\cos[(k_x - k_z)a/2] - 2t_{p\pi}\cos[(k_x + k_z)a/2] - E_F + E_0. \quad (2)$$

The TB coupling parameters $t_{p\sigma} = -1.9$ eV along and $t_{p\pi} = 0.35$ eV perpendicular to the Te chains [Fig. 1(a)] have been established by ARPES experiments [20,22,24]. $E_F = -2t_{p\sigma}\sin(\pi/8)$ and $|\vec{q}| = 0.685(2\pi/a)$ are constant. The in-plane lattice spacing is given by $a = 4.34$ Å [15]. The band dispersion is extracted by fitting a Gaussian function to the

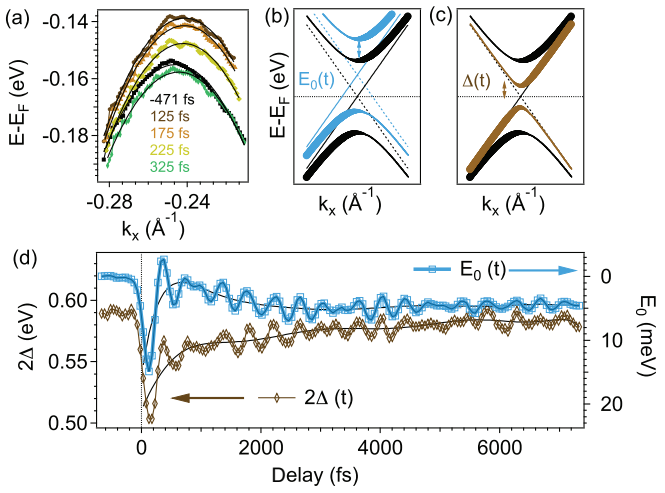

FIG. 2. (Color online) (a) Measured dispersion of the occupied Te-5p band for selected delays (*markers*) and transient TB fits (*lines*). Sketched effect of (b) a transient rigid energy shift $E_0(t)$ and (c) a change in the CDW gap $\Delta(t)$ on the band dispersion. (d) The $2\Delta(t)$ and $E_0(t)$ with smooth backgrounds (*black lines*) of a tenth-order polynomial indicated.

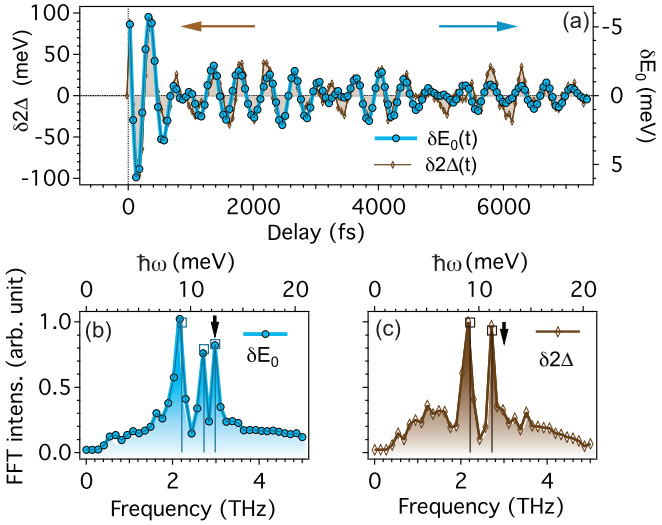

FIG. 3. (Color online) (a) Residuals of the polynomial background fit shown in Fig. 2(d). (b) and (c) Fourier transformation (FT) of (a). The *vertical lines* and *markers* at $\Omega_1 = 2.19(1)$, $\Omega_2 = 2.69(1)$, and $\Omega_3 = 2.98(1)$ THz indicate mode frequencies and amplitudes independently obtained from fitting damped cosine functions, see Supplemental Material [35].

spectra as a function of $\vec{k}$ and yield the data points in Fig. 1(e). Equations (1) and (2) are combined and simultaneously fitted to the extracted dispersion above and below E_F at -25 fs as shown in Fig. 1(e). The rigid energy shift $E_0 = 0$ is kept fixed, and the only free fit parameter is Δ. This yields $2\Delta = 0.59(1)$ eV, which is identical to the value derived from the difference of upper and lower band energies at -25 fs.

After having established that the TB model is well suited to describe the gapped dispersion near E_F, it is applied to the occupied band for all delays as shown in Fig. 2(a) with $\Delta(t)$ and $E_0(t)$ now being free time-dependent fit parameters. The low excitation regime allows for holding the TB parameters $t_{p\sigma}$ and $t_{p\pi}$ constant. $\Delta(t)$ leads to momentum-dependent modulations in the spectra and is naturally sensitive to the AM [10] as illustrated in Fig. 2(c). In contrast, $E_0(t)$ is a momentum-independent energy shift of the whole band structure as sketched in Fig. 2(b). As we will show, these parameters capture the two types of modes observed.

Results for $2\Delta(t)$ and $E_0(t)$ are shown in Fig. 2(d). The magnitude of $E_0(t)$ amounts to a few meV and is much smaller than the changes in $2\Delta(t)$, which are on the order of several 10 meV. Within the pump pulse duration, 2Δ drops by 15%, yet the charge order is only perturbed and not destroyed, see Supplemental Material [35]. After $\sim$3 ps, the system has thermalized at a reduced gap size, which agrees with the time scale of the suppression of the structural order parameter satellite observed in time-resolved electron diffraction [36,37].

The pronounced beating patterns of $2\Delta(t)$ and $E_0(t)$ exhibit an oscillatory response with similar yet distinct frequencies. For a more detailed analysis smooth backgrounds (tenth-order polynomials) are subtracted, and the residuals $\delta 2\Delta(t)$ and $\delta E_0(t)$ are plotted in Fig. 3(a). Analysis via Fourier transformation (FT) of $\delta 2\Delta(t)$ reveals two dominant frequencies at $\Omega_1 = 2.2(1)$ and $\Omega_2 = 2.7(1)$ THz as shown in Fig. 3(c). In contrast, the oscillatory response and particularly the beating pattern of $\delta E_0(t)$ differs from $\delta 2\Delta(t)$. In addition to Ω_1 and Ω_2, the FT of $\delta E_0(t)$ exhibits a third pronounced peak at $\Omega_3 = 3.0(1)$ THz, marked by a vertical arrow in Fig. 3(b). These findings are robust regardless of the background subtraction, see Supplemental Material [35]. Fitting damped cosine functions to $\delta 2\Delta(t)$ and $\delta E_0(t)$, see Supplemental Material [35], yields the same frequencies albeit with higher resolution as indicated in Fig. 3.

The mode at Ω_1 is identified as a previously observed AM of RTe$_3$. As sketched in Fig. 4(a), coherent in-plane atomic motions modulate the lattice distortion Δz and thus directly affect Δ. This assignment is supported by comparing frequency Ω_1 to the soft mode observed in temperature-dependent transient optical reflectivity [7,27], temperature-dependent Raman spectroscopy [19,25,26], and temperature- and fluence-dependent trARPES [4,29,30].

The mode at Ω_2 is missing at the zone center of the frozen phonon calculations, suggesting it originates either from a normal-state optical or from an acoustic branch which is renormalized by coupling to the charge modulation at $\vec{q}$. A finite projection of the ionic motion on the lattice displacement Δz associated with the CDW then naturally explains its presence in $\Delta(t)$ and the temperature-dependent softening in Refs. [26,27]. We thus assign Ω_2 as a second AM.

The mode at Ω_3 is assigned to an out-of-plane A_{1g} phonon, which is not related to the CDW by comparison to frozen phonon calculations and transient reflectivity [27]. The calculated displacement of the Te atoms is sketched in Fig. 4(c). The response of the Te-5p band is remarkably mode dependent; Ω_3 mainly affects E_0 and has a much smaller influence on Δ, even though Ω_3 involves the motion of the Te atoms, which form the CDW bands. However, the out-of-plane motion couples only weakly to the charge order with correspondingly small influence on the order parameter Δ.

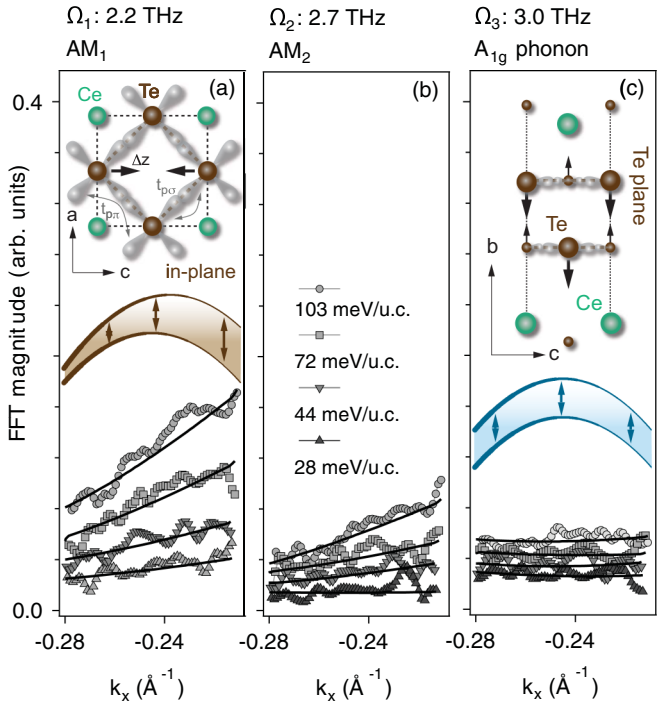

FIG. 4. (Color online) Mode-dependent modulations of the Te-5p bands (*markers*) by the three dominant modes is derived from momentum-dependent FT amplitudes for deposited energies of 28–103 meV per unit cell. *Solid lines* are obtained from the corresponding TB fits of the transient Te-5p bands, see Supplemental Material [35]. (a) The AM at $\Omega_1 = 2.2$ THz modulates the in-plane lattice displacement Δz and leads to a strongly momentum- and fluence-dependent response. (b) The AM at $\Omega_2 = 2.7(1)$ THz exhibits a weaker momentum and fluence dependence, which indicates a weaker influence on the in-plane CDW. (c) The out-of-plane A_{1g} mode at $\Omega_3 = 3$ THz only shifts the band rigidly as it does not couple to the in-plane charge order.

To further investigate this explanation for mode-dependent coupling we plot FT amplitudes for all three modes in Fig. 4 as a function of fluence and momentum. These are derived from an FT analysis of the oscillatory binding energies, which have been extracted from transient spectra as a function of $\vec{k}$, see Supplemental Material [35]. The influence on the dispersion is illustrated in Figs. 4(a) and 4(c). The AM at Ω_1 is strongly fluence and momentum dependent as expected for a reduction of Δ. The AM at Ω_2 exhibits a qualitatively similar behavior albeit of smaller magnitude. This is consistent with a smaller coupling between the phonon with the charge density or a smaller projection of the ionic motion on the lattice distortion Δz.

In contrast, the out-of-plane A_{1g} phonon at Ω_3 causes a strikingly k-independent shift, which is only weakly dependent on fluence. This suggests a small fluence-dependent atomic displacement $\mu(t)$ and a constant deformation potential $D_{5p}(\vec{k})$ that explains the rigid energy shift via $E_0(t) \sim D_{5p}(\vec{k})\mu(t)$ [38,39]. We confirm the approximation of a k-independent deformation potential by DFT calculations for atomic displacements μ of up to 0.13 Å, shown in the Supplemental Material Ref. [35].

To summarize, trARPES measurements on $CeTe_3$ reveal a CDW gap size of $2\Delta = 0.59$ eV. Coherent excitations of two AMs at $\Omega_1 = 2.2$ and at $\Omega_2 = 2.7$ THz and a generic A_{1g} phonon at $\Omega_3 = 3$ THz are identified by fits of a time-dependent model dispersion and comparison to normal-state frozen phonon calculations. The out-of-plane A_{1g} phonon leads to small rigid shifts in the entire Te-5p band but does not affect Δ. In contrast, Ω_1 and Ω_2 result in pronounced changes in Δ. We point out that our k-dependent analysis combined with low excitation densities is key to identifying and assigning AMs. We have generalized our approach and introduced a model-free evaluation (Fig. 4), which can be applied to materials where a detailed description of the band dispersion may not be available. More specifically, our approach can be transferred to charge ordering in striped cuprates [40], which has identical symmetry to RTe_3 [41].

We acknowledge helpful discussions with B. Moritz, S. Gerber, and R. Hackl. This work was supported by the U.S. Department of Energy, Office of Science, Basic Energy Sciences, Materials Sciences and Engineering Division under Contract No. DE-AC02-76SF00515. D.L. acknowledges support from the Swiss National Science Foundation, under Fellowship No. P300P2_151328. S.-L.Y. acknowledges support from the Stanford Graduate Fellowship. The work by A.F.K. was supported by the Laboratory Directed Research and Development Program of Lawrence Berkeley National Laboratory under U.S. Department of Energy Contract No. DE-AC02-05CH11231.

[1] E. Fradkin and S. A. Kivelson, Nat. Phys. **8**, 864 (2012).

[2] K. Sokolowski-Tinten, C. Blome, J. Blums, A. Cavalleri, C. Dietrich, A. Tarasevitch, I. Uschmann, E. Förster, M. Kammler, M. H. von Hoegen *et al.*, Nature (London) **422**, 287 (2003).

[3] D. M. Fritz, D. A. Reis, B. Adams, R. A. Akre, J. Arthur, C. Blome, P. H. Bucksbaum, A. L. Cavalieri, S. Engemann, S. Fahy *et al.*, Science **315**, 633 (2007).

[4] F. Schmitt, P. S. Kirchmann, U. Bovensiepen, R. G. Moore, L. Rettig, M. Krenz, J.-H. Chu, N. Ru, L. Perfetti, D. H. Lu *et al.*, Science **321**, 1649 (2008).

[5] M. Eichberger, H. Schäfer, M. Krumova, M. Beyer, J. Demsar, H. Berger, G. Moriena, G. Sciaini, and R. J. D. Miller, Nature (London) **468**, 799 (2010).

[6] H. Schäfer, V. V. Kabanov, M. Beyer, K. Biljakovic, and J. Demsar, Phys. Rev. Lett. **105**, 066402 (2010).

[7] R. Yusupov, T. Mertelj, V. V. Kabanov, S. Brazovskii, P. Kusar, J.-H. Chu, I. R. Fisher, and D. Mihailovic, Nat. Phys. **6**, 681 (2010).

[8] T. Rohwer, S. Hellmann, M. Wiesenmayer, C. Sohrt, A. Stange, B. Slomski, A. Carr, Y. Liu, L. M. Avila, M. Kalläne *et al.*, Nature (London) **471**, 490 (2011).

[9] S. Hellmann, T. Rohwer, M. Kalläne, K. Hanff, C. Sohrt, A. Stange, A. Carr, M. M. Murnane, H. C. Kapteyn, L. Kipp *et al.*, Nat. Commun. **3**, 1069 (2012).
[10] G. Grüner, *Density Waves in Solids* (Addison-Wesley, Reading, MA, 1994), Vol. 89.
[11] E. D. DiMasi, M. C. Aronson, J. F. Mansfield, B. Foran, and S. Lee, Phys. Rev. B **52**, 14516 (1995).
[12] H. J. Kim, C. D. Malliakas, A. T. Tomic, S. H. Tessmer, M. G. Kanatzidis, and S. J. L. Billinge, Phys. Rev. Lett. **96**, 226401 (2006).
[13] A. Sacchetti, L. Degiorgi, T. Giamarchi, N. Ru, and I. R. Fisher, Phys. Rev. B **74**, 125115 (2006).
[14] N. Ru and I. R. Fisher, Phys. Rev. B **73**, 033101 (2006).
[15] N. Ru, C. L. Condron, G. Y. Margulis, K. Y. Shin, J. Laverock, S. B. Dugdale, M. F. Toney, and I. R. Fisher, Phys. Rev. B **77**, 035114 (2008).
[16] A. Sacchetti, C. L. Condron, S. N. Gvasaliya, F. Pfuner, M. Lavagnini, M. Baldini, M. F. Toney, M. Merlini, M. Hanfland, J. Mesot *et al.*, Phys. Rev. B **79**, 201101(R) (2009).
[17] A. Tomic, Z. Rak, J. P. Veazey, C. D. Malliakas, S. D. Mahanti, M. G. Kanatzidis, and S. H. Tessmer, Phys. Rev. B **79**, 085422 (2009).
[18] A. Banerjee, Y. Feng, D. M. Silevitch, J. Wang, J. C. Lang, H.-H. Kuo, I. R. Fisher, and T. F. Rosenbaum, Phys. Rev. B **87**, 155131 (2013).
[19] H.-M. Eiter, M. Lavagnini, R. Hackl, E. A. Nowadnick, A. F. Kemper, T. P. Devereaux, J.-H. Chu, J. G. Analytis, I. R. Fisher, and L. Degiorgi, Proc. Natl. Acad. Sci. USA **110**, 64 (2013).
[20] R. G. Moore, V. Brouet, R. He, D. H. Lu, N. Ru, J.-H. Chu, I. R. Fisher, and Z.-X. Shen, Phys. Rev. B **81**, 073102 (2010).
[21] G.-H. Gweon, J. D. Denlinger, J. A. Clack, J. W. Allen, C. G. Olson, E. D. DiMasi, M. C. Aronson, B. Foran, and S. Lee, Phys. Rev. Lett. **81**, 886 (1998).
[22] V. Brouet, W. L. Yang, X. J. Zhou, Z. Hussain, N. Ru, K. Y. Shin, I. R. Fisher, and Z. X. Shen, Phys. Rev. Lett. **93**, 126405 (2004).
[23] H. Komoda, T. Sato, S. Souma, T. Takahashi, Y. Ito, and K. Suzuki, Phys. Rev. B **70**, 195101 (2004).
[24] V. Brouet, W. L. Yang, X. J. Zhou, Z. Hussain, R. G. Moore, R. He, D. H. Lu, Z.-X. Shen, J. Laverock, S. B. Dugdale *et al.*, Phys. Rev. B **77**, 235104 (2008).
[25] M. Lavagnini, M. Baldini, A. Sacchetti, D. D. Castroa, B. Delley, R. Monnier, J.-H. Chu, N. Ru, I. R. Fisher, P. Postorino *et al.*, Phys. Rev. B **78**, 201101(R) (2008).
[26] M. Lavagnini, H.-M. Eiter, L. Tassini, B. Muschler, R. Hackl, R. Monnier, J.-H. Chu, I. R. Fisher, and L. Degiorgi, Phys. Rev. B **81**, 081101 (2010).
[27] R. V. Yusupov, T. Mertelj, J.-H. Chu, I. R. Fisher, and D. Mihailovic, Phys. Rev. Lett. **101**, 246402 (2008).
[28] R. Y. Chen, B. F. Hu, T. Dong, and N. L. Wang, Phys. Rev. B **89**, 075114 (2014).
[29] F. Schmitt, P. S. Kirchmann, U. Bovensiepen, R. G. Moore, J.-H. Chu, D. H. Lu, L. Rettig, M. Wolf, I. R. Fisher, and Z.-X. Shen, New J. Phys. **13**, 063022 (2011).
[30] L. Rettig, J.-H. Chu, I. R. Fisher, U. Bovensiepen, and M. Wolf, Faraday Discuss. **171**, 299 (2014).
[31] J. A. Sobota, S. Yang, J. G. Analytis, Y. L. Chen, I. R. Fisher, P. S. Kirchmann, and Z.-X. Shen, Phys. Rev. Lett. **108**, 117403 (2012).
[32] S.-L. Yang, J. A. Sobota, P. S. Kirchmann, and Z.-X. Shen, Appl. Phys. A **116**, 85 (2014).
[33] P. Giannozzi, J. Phys.: Condens. Matter **21**, 395502 (2009).
[34] J. P. Perdew, K. Burke, and M. Ernzerhof, Phys. Rev. Lett. **77**, 3865 (1996).
[35] See Supplemental Material at http://link.aps.org/supplemental/10.1103/PhysRevB.91.201106 for DFT calculations for atomic displacements.
[36] T.-R. T. Han, Z. Tao, S. D. Mahanti, K. Chang, C.-Y. Ruan, C. D. Malliakas, and M. G. Kanatzidis, Phys. Rev. B **86**, 075145 (2012).
[37] Z. Tao, T.-R. T. Han, and C.-Y. Ruan, Phys. Rev. B **87**, 235124 (2013).
[38] F. S. Khan and P. B. Allen, Phys. Rev. B **29**, 3341 (1984).
[39] J. Faure, J. Mauchain, E. Papalazarou, M. Marsi, D. Boschetto, I. Timrov, N. Vast, Y. Ohtsubo, B. Arnaud, and L. Perfetti, Phys. Rev. B **88**, 075120 (2013).
[40] J. M. Tranquada, B. J. Sternlieb, J. D. Axe, Y. Nakamura, and S. Uchida, Nature (London) **375**, 561 (1995).
[41] H. Yao, J. A. Robertson, E.-A. Kim, and S. A. Kivelson, Phys. Rev. B **74**, 245126 (2006).